N-Acetyl-Seryl-Aspartyl-Lysyl-Proline Ameliorates the Progression of Renal Dysfunction and Fibrosis in WKY Rats with Established Anti–Glomerular Basement Membrane Nephritis

Mitsugu Omata,* Hajime Taniguchi,* Daisuke Koya,† Keizo Kanasaki,‡ Rumiko Sho,*
Yoshimi Kato,* Ryoji Kojima,§ Masakazu Haneda,‖ and Norio Inomata*

*Biomedical Research Laboratories, Daiichi Asubio Pharma Co., Ltd., Osaka; †Department of Endocrinology and Metabolism, Kanazawa Medical University, Ishikawa; ‡Department of Medicine, Shiga University of Medical Science, Shiga; §Laboratory of Analytical Pharmacology, Faculty of Pharmacy, Meijo University, Nagoya; and ‖Second Department of Internal Medicine, Asahikawa Medical College, Asahikawa, Japan

N-acetyl-seryl-aspartyl-lysyl-proline (Ac-SDKP), which is hydrolyzed by angiotensin-converting enzyme, is a natural regulator of hematopoiesis. Here it is shown that Ac-SDKP inhibits TGF-β action in mesangial cells. Because TGF-β is thought to play a pivotal role in the development and progression of glomerulonephritis, the therapeutic effects of Ac-SDKP on an established model of renal dysfunction and histologic alteration in Wistar-Kyoto rats with anti–glomerular basement membrane nephritis was examined. Fourteen days after the induction of anti–glomerular basement membrane nephritis, the rats were treated subcutaneously with Ac-SDKP at a dose of 1 mg/kg per d for 4 wk. Treatment with Ac-SDKP significantly improved proteinuria and renal dysfunction, including increased plasma blood urea nitrogen and creatinine levels and decreased creatinine clearance. Histologic examination showed severe glomerulosclerosis and interstitial fibrosis in the vehicle-treated rats, whereas these histologic injuries were significantly ameliorated in rats that were treated with Ac-SDKP. The histologic improvements were accompanied by the suppression of gene and protein expression of fibronectin, interstitial collagen, and TGF-β1 in the nephritic kidney. Furthermore, treatment with Ac-SDKP resulted in the inhibition of Smad2 phosphorylation, an increase in Smad7 expression in the kidney, and reduction of macrophage accumulation into the glomeruli and tubulointerstitium in nephritic rats. In conclusion, Ac-SDKP significantly ameliorated the progression of renal dysfunction and fibrosis even after the establishment of nephritis. The inhibitory effect of Ac-SDKP was mediated in part by the inhibition of TGF-β/Smad signal transduction and the inflammatory response. These findings suggest that Ac-SDKP treatment may be a novel and useful therapeutic strategy for the treatment of progressive renal diseases.

It has been reported that more than 20 million people worldwide have lost half of their renal function or have shown overt proteinuria (1). The number of patients who have ESRD or must undergo chronic renal dialysis therapy is ever increasing (2,3). The end-stage lesions, such as glomerulosclerosis and tubulointerstitial fibrosis, are characterized by the advanced loss of renal cells and excessive accumulation of extracellular matrix (ECM), including fibronectin and collagens; these lesions represent a common structure independent of the primary underlying disease (4,5). Although most patients who have chronic kidney disease (CKD) have been treated with several pharmacotherapies before reaching end-stage renal failure, no currently available treatment is effective in halting the loss of residual renal function and the progression of renal fibrosis (6–8). Therefore, the development of novel therapeutic agents that interrupt the uncontrollable fibrotic response to renal injury has been eagerly anticipated.

N-acetyl-seryl-aspartyl-lysyl-proline (Ac-SDKP) is an endogenous tetrapeptide that possesses a regulatory effect on the proliferation of hematopoietic stem cells (9). Ac-SDKP, which is normally present in plasma and mononuclear cells, is degraded in the circulation by angiotensin I–converting enzyme (ACE) (10). In some *in vivo* studies, Ac-SDKP prevented collagen deposition in the left ventricle and kidneys in a hypertensive rat model (11,12) and reversed cardiac inflammation and fibrosis in rats with heart failure induced by myocardial infarction (13). More recently, we also found that treatment with Ac-SDKP prevents the renal insufficiency and glomerular mesangial matrix expansion observed in type 2 diabetic db/db mice (14). In some *in vitro* studies, Ac-SDKP has been shown to suppress the proliferation of renal fibroblasts (15) and to inhibit DNA and collagen synthesis in cardiac fibroblasts (16). We have shown that Ac-SDKP is able to inhibit the TGF-β–induced expression of plasminogen activator inhibitor-1 and α2-type I collagen through the suppression of Smad signaling in mesangial cells

(17). Because profibrotic cytokine TGF-β is thought to play a pivotal role in the progression of glomerulonephritis and tubulointerstitial fibrosis (18,19), we investigated the ability of Ac-SDKP to inhibit TGF-β action and improve renal fibrosis and dysfunction in a glomerulosclerosis model. Most patients who receive a diagnosis of CKD already have renal dysfunction accompanied by some degree of fibrotic lesions in the kidneys. Therefore, we administered Ac-SDKP 2 wk after nephritis induction in our rat model, a time point after the development of renal dysfunction and pathologic changes. We found that Ac-SDKP significantly ameliorated the progression of renal dysfunction and fibrosis even after the establishment of nephritis. The inhibitory effects of Ac-SDKP were mediated in part by the inhibition of TGF-β/Smad signal transduction and inflammatory responses, such as monocyte/macrophage accumulation.

Materials and Methods

Experimental Protocol

All animal experiments were approved by the Animal Care and Ethics Committee of Daiichi Asubio Pharma. Male Wistar-Kyoto (WKY) rats were purchased from Charles River Japan (Kanagawa, Japan). On day 0, 0.025 ml of rabbit anti-rat glomerular basement membrane (GBM) serum (20) was injected intravenously into 18 7-wk-old rats. Fourteen days after the induction of nephritis, urine samples were collected for 24 h to measure of urinary protein excretion. Four rats were selected randomly and killed on day 14. After examination of the urinary protein excretion, the remaining rats were randomly assigned to two groups: Rats anti-GBM nephritis, which were given no treatment ($n = 7$), and rats that had anti-GBM nephritis and were treated with 1 mg/kg per d Ac-SDKP ($n = 7$). An osmotic minipump (Alzet2 ML4, Alzet, Cupertino, CA) was implanted subcutaneously in the neck to deliver either Ac-SDKP or vehicle, saline plus 0.01 N acetic acid. The dosage of Ac-SDKP and the route of administration were selected on the basis of previously described procedures (11,14). Ac-SDKP was infused subcutaneously for 4 wk. Age-matched male WKY rats without nephritis were used as normal controls. Serial blood samples were taken *via* tail-vein puncture under light anesthesia induced by isoflurane inhalation on days 0, 14, 21, 28, and 35. Twenty-four-hour urine samples for the measurement of proteinuria were collected during the same period. At 42 d after nephritis induction, the animals received perfusion of sterile saline administered to the thoracic aorta under anesthesia (50 mg/kg pentobarbital). The renal cortex was dissected from the left kidney, immediately frozen in liquid nitrogen, and stored at $-80°C$ until further analysis. The right kidney was excised and immersed in 4% paraformaldehyde for histologic examination.

Determination of Blood and Urine Parameters

Urinary protein concentrations were determined using the method of Kingsbury *et al.* (21). Plasma (Pcr) and urinary (Ucr) creatinine and blood urea nitrogen (BUN) levels were determined using an autoanalyzer (HITACHI clinical analyzer 7070; Hitachi High-Technologies Co., Tokyo, Japan). For avoidance of errors from incomplete urine collection, urinary protein excretion was normalized to the levels of urinary creatinine. Creatinine clearance (Ccr) was calculated using the standard formula Ccr = Ucr × urine volume/Pcr and was expressed as ml/min per 100 g body wt.

Histologic Examination

The longitudinally bisected kidney was embedded in paraffin, sectioned, and stained with periodic acid-Schiff and Masson's trichrome reagents. The sections were evaluated by two independent observers who were unaware of the origin of the slides. For determination of glomerulosclerosis, 100 glomeruli were randomly selected in cross-sections that were obtained from each rat. Glomerulosclerosis, which was defined as glomeruli exhibiting adhesion of the capillary tuft to the Bowman's capsule, capillary obliteration, mesangial expansion, or fibrotic crescents, was graded semiquantitatively as follows: 0, normal; 1, 0 to 25% of the glomerular area affected; 2, 25 to 50% affected; 3, 50 to 75% affected; and 4, 75 to 100% affected (22). The degree of glomerulosclerosis was expressed as the glomerulosclerosis index (GSI). The GSI of a whole kidney was obtained by averaging the scores from 100 glomeruli in one section. Furthermore, scores that were obtained by two independent investigators were averaged. For quantification of tubulointerstitial fibrosis, 50 fields were randomly selected from the cortical region and were analyzed under high-power magnification ($\times 400$). Fibrotic areas in the interstitium, which were stained blue, were identified on the digital images using a computer-aided manipulator (LuminaVision; Mitani Co., Fukui, Japan). The percentage of fibrotic area was calculated. Glomeruli and large vessels were excluded from analysis. The deposition of interstitial collagen was evaluated by staining with picrosirius red. Fifty fields were randomly selected from the cortical region and analyzed under high-power magnification ($\times 400$). Areas of collagen deposition in the interstitium, which were stained red, were identified on digital images using LuminaVision. The percentage of red area was calculated.

Table 1. Primers used for PCR[a]

Gene	Forward	Reverse
GAPDH	5′-TGCACCACCAACTGCTTAG-3′	5′-GGATGCAGGGATGATGTTC-3′
Type I collagen	5′-CCGATGGATTCCAGTTCGA-3′	5′-AGGTCAGCTGGATAGCGACAT-3′
Type III collagen	5′-CCATTGCTGGAGTTGGAGGT-3′	5′-GTGAAGACATGATCTCCTCAGTGTTG-3′
Fibronectin	5′-GCAACGTGTTATGACGACGG-3′	5′-TGCGGCAGTTGTCACAGC-3′
TGF-β1	5′-AGTCCCAAACGTCGAGGTGA-3′	5′-AGGTGTTGAGCCCTTTCCAG-3′
TNF-α	5′-ATCGGTCCCAACAAGGAGGA-3′	5′-TGGTGGTTTGCTACGACGTG-3′
IL-1β	5′-CAACAAGTGGTATTCTCCATGAGC-3′	5′-GGTGTGCCGTCTTTCATCAC-3′
MCP-1	5′-GCTGCTACTCATTCACTGGCAA-3′	5′-CTGCTGCTGGTGATTCTCTTGT-3′
ICAM-1	5′-GGAGCCAATTTCTCATGCTTCA-3′	5′-AGATCGAAAGTCCGGAGCTG-3′

[a]GAPDH, glyceraldehyde-3-phosphate dehydrogenase; ICAM-1, intercellular adhesion molecule-1; MCP, monocyte chemoattractant protein-1.
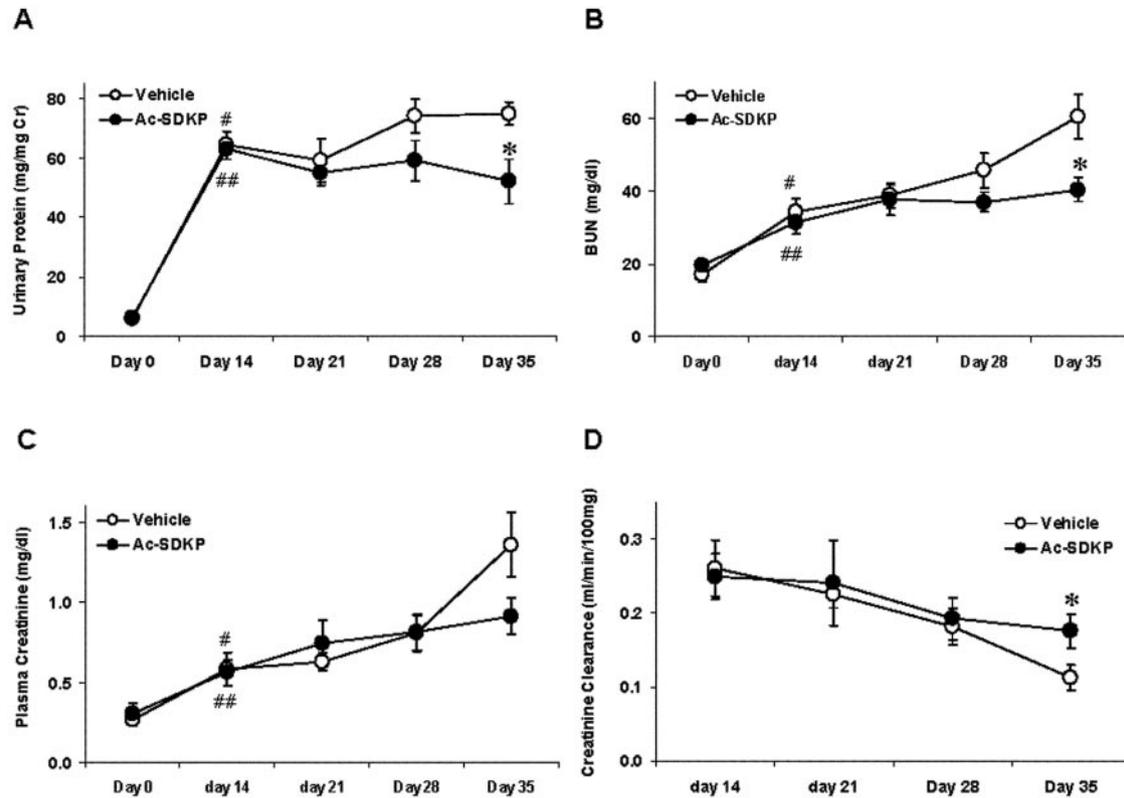
Figure 1. Therapeutic effects of N-acetyl-seryl-aspartyl-lysyl-proline (Ac-SDKP) on urinary protein (A), blood urea nitrogen (B), plasma creatinine (C), and creatinine clearance (D) in rats with anti–glomerular basement membrane (ant-GBM) nephritis. Each symbol represents the mean ± SEM of seven rats that were treated with vehicle (○) or 1 mg/kg per d Ac-SDKP (●). Statistical significance is based on the *t* test: *$P < 0.05$ *versus* the same time point of the vehicle group; #$P < 0.01$ for the vehicle group *versus* day 0; ##$P < 0.01$ for the Ac-SDKP–treated group *versus* day 0.

Immunohistochemistry

Immunohistochemical staining for rat monocyte/macrophage (ED-1) was performed using an avidin-biotin complex staining method (VEC-TASTAIN *Elite* ABC kit; Vector Laboratory, Burlingame, CA). After deparaffinization, slides were placed in 0.01 M citrate and heated in a microwave oven at 2450 MHz and 800 W for 10 min. The slides were incubated in normal blocking serum for 6 h followed by overnight incubation at 4°C with a monoclonal mouse antibody against rat macrophages (ED-1) (Serotec, Oxford, UK). Endogenous peroxidase was inactivated by incubation for 10 min with 3% H_2O_2, and a biotinylated anti-mouse antibody was added for 45 min at room temperature. After washing, VECTAIN *elite* ABC/Reagent was added for 30 min at room temperature. The color reaction was developed with 3,3′-diaminobenzidine and counterstained with hematoxylin.

The accumulation of monocytes/macrophages into the renal tissue was evaluated by assessing the number of ED-1–positive cells. The number of ED-1–positive cells in the renal cortex was determined by observation of 50 randomly selected glomeruli or cortical interstitial areas in each cross-section.

Western Blot Analysis

The expression levels of fibronectin, Smad2, phosphorylated Smad2, and Smad7 were examined by Western blotting. Briefly, renal cortex tissue was homogenized in 0.5 ml of ice-cold lysis buffer (23). Samples were centrifuged at 12,000 × *g* for 10 min, and the supernatants were used for the assay. After mixing with SDS-PAGE sample buffer and boiling for 5 min, samples (20 μg/lane) were electrophoresed on 7.5%

SDS polyacrylamide gels and transferred to polyvinylidene difluoride membranes for 1.5 h at 180 mA. Membranes were blocked for 1 h with Block-Ace (Daihippon, Japan) and incubated with primary antibody overnight at 4°C. Primary antibodies that were used in this study included anti-rat fibronectin antibody (1:300 dilution; Chemicon International, Temecula, CA), anti-phosphorylated Smad2 antibody (1:1000 dilution; Cell Signaling Technology, Danvers, MA), anti-Smad2 antibody (1:1000 dilution; Cell Signaling Technology), and anti-Smad7 antibody (1:200 dilution; Santa Cruz Biotechnology, Santa Cruz, CA) overnight at 4°C. After washing, membranes were incubated with horseradish peroxidase–conjugated anti-rabbit IgG for 1 h. Western blots were visualized using the enhanced chemiluminescence system (LumiGLO Reagent; Cell signaling Technology), which was captured on x-ray film. The same membranes were stripped and reprobed with anti–β-actin antibody (1:200 dilution; Santa Cruz Biotechnology) to confirm equal loading.

Real-Time Reverse Transcription–PCR

Total RNA was isolated with the use of a commercial kit (RNase mini kit; Qiagen, Valencia, CA). cDNA was generated from 1.5 μg of total RNA and oligo(dT) primers using the SuperScript First-Strand Synthesis System (Invitrogen, Carlsbad, CA) for reverse transcription–PCR according to the manufacturer's protocol. Quantitative real-time Taq-Man PCR was performed in a 40-μl reaction volume that contained 1 μl of cDNA template, 20 μl of Universal Master Mixture (Applied Biosystems, Foster City, CA), 100 nM each of sense and antisense primers, and the TaqMan probe. The PCR amplification profiles included an initial
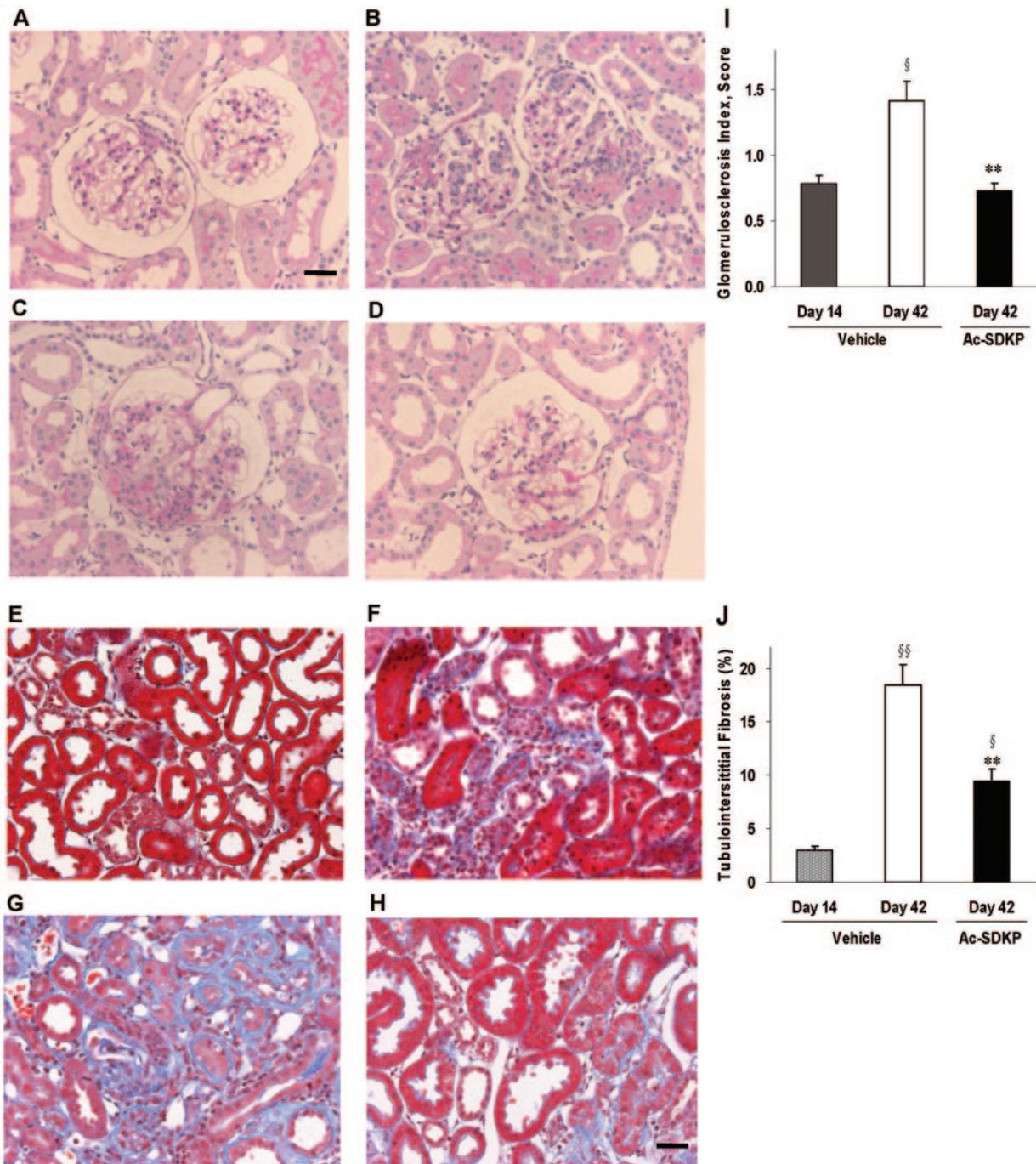
Figure 2. Effects of Ac-SDKP on glomerular injury and tubulointerstitial fibrosis in rats with anti-GBM nephritis. Representative photomicrographs of periodic acid-Schiff–stained glomerulosclerotic lesions in renal sections from normal rats (A), day 14 nephritic rats (B), day 42 nephritic rats that were treated with vehicle (C), and day 42 nephritic rats that were treated with 1 mg/kg per d Ac-SDKP (D). Bar = 30 μm. Glomerulosclerosis was scored on the sclerosis index (I). Each column shows the data from day 14 nephritic rats that were treated with vehicle (▨), day 42 nephritic rats that were treated with vehicle (□), and day 42 nephritic rats that were treated with 1 mg/kg per d Ac-SDKP (■). Each column represents the mean ± SEM of four rats on day 14 in the vehicle group or seven rats on day 42 in the vehicle and Ac-SDKP groups. Statistical significance is based on the Mann-Whitney U test: [§]$P < 0.05$ *versus* day 14 in the nephritic rats; **$P < 0.01$ *versus* day 42 in the vehicle group. (E through H) Representative photomicrographs of tubular lesions in renal sections from normal rats (E), day 14 nephritic rats (F), day 42 nephritic rats that were treated with vehicle (G), and day 42 nephritic rats that were treated with 1 mg/kg per d Ac-SDKP (H). (J) The percentage of the entire field that was fibrotic and stained blue was calculated. Each column shows data from day 14 nephritic rats that were treated with vehicle (▨), day 42 nephritic rats that were treated with vehicle (□), and day 42 nephritic rats that were treated with 1 mg/kg per d Ac-SDKP (■). Each column represents the mean ± SEM of four rats on day 14 in the vehicle group or seven rats on day 42 in the vehicle and Ac-SDKP groups. Statistical significance: [§]$P < 0.05$, [§§]$P < 0.01$ *versus* day 14 in the nephritic rats by Dunnett test; **$P < 0.01$ *versus* day 42 in the vehicle group by the t test.

incubation at 50°C for 2 min, denaturation at 95°C for 10 min, and 40 to 45 cycles of 95°C for 15 s and 60°C for 1 min. The specific primers are listed in Table 1. Reactions were performed in duplicate. All data are presented after normalization to the glyceraldehyde-3-phosphate dehydrogenase expression observed in the same sample.

Measurement of TGF-β1 Protein

Renal cortex tissue was homogenized in 0.5 ml of ice-cold lysis buffer. Samples were centrifuged at 12,000 × g for 10 min, and the supernatants were used for the assay. TGF-β1 levels were determined using an ELISA kit (R&D Systems, Minneapolis, MN) according to the manufacturer's methods. As this activity represents active TGF-β1, acid activation of the samples was required to convert the latent TGF-β1 to the active form and determine the total level of TGF-β1. A portion of the renal tissue homogenate was assayed for total protein using a BCA protein assay kit (Pierce, Rockford, IL). The total TGF-β1 levels were expressed as TGF-β1 levels per total protein levels in the tissue homogenate.

Plasma Level of Ac-SDKP

At the end of the experiment, blood was collected from the abdominal aorta in a tube that contained heparin and captopril, an ACE inhibitor, at a final concentration of 10 μM. Samples were centrifuged at 8 000 × g for 10 min at 4°C. The recovered plasma was stored at −80°C until the Ac-SDKP assay was performed. Plasma Ac-SDKP was quantified with a competitive enzyme immunoassay (SPI-BIO, Montigny le Bretonneux, France).

Statistical Analyses

Results were presented as the mean ± SEM. Comparisons between two groups were performed using either the t test, when the data were normally distributed, or the Mann-Whitney U test, when the observations showed considerable variability. The comparison of semiquantitative analyses, such as GSI scores, was also evaluated by the Mann-Whitney U test. Differences among three or more groups were evaluated using two-way ANOVA, followed by Dunnett test. $P < 0.05$ was considered to be statistically significant.

Results

Renal Dysfunction

Fourteen days after the induction of nephritis, proteinuria and plasma levels of BUN and creatinine were markedly increased compared with the levels observed on day 0. After the observation at day 14, animals were randomly assigned to the vehicle-treated group or the Ac-SDKP–treated group. In the vehicle-treated group, proteinuria remained at high levels on days 21, 28, and 35. In addition, the plasma BUN and creatinine levels in the vehicle-treated group showed a tendency to increase in a time-dependent manner. On day 35, the proteinuria in the Ac-SDKP–treated group (52.1 ± 7.5 mg/mg Cr) was significantly lower than that in the vehicle-treated group (74.8 ± 3.8 mg/mg Cr; Figure 1A). The BUN level in the Ac-SDKP–treated group on day 35 was significantly lower than that in the vehicle-treated group by 33.2% (Figure 1B). The plasma creatinine level was reduced by Ac-SDKP treatment (32.6% reduction relative to vehicle treatment), consistent with the BUN level (Figure 1C). Furthermore, creatinine clearance on day 35 in the Ac-SDKP–
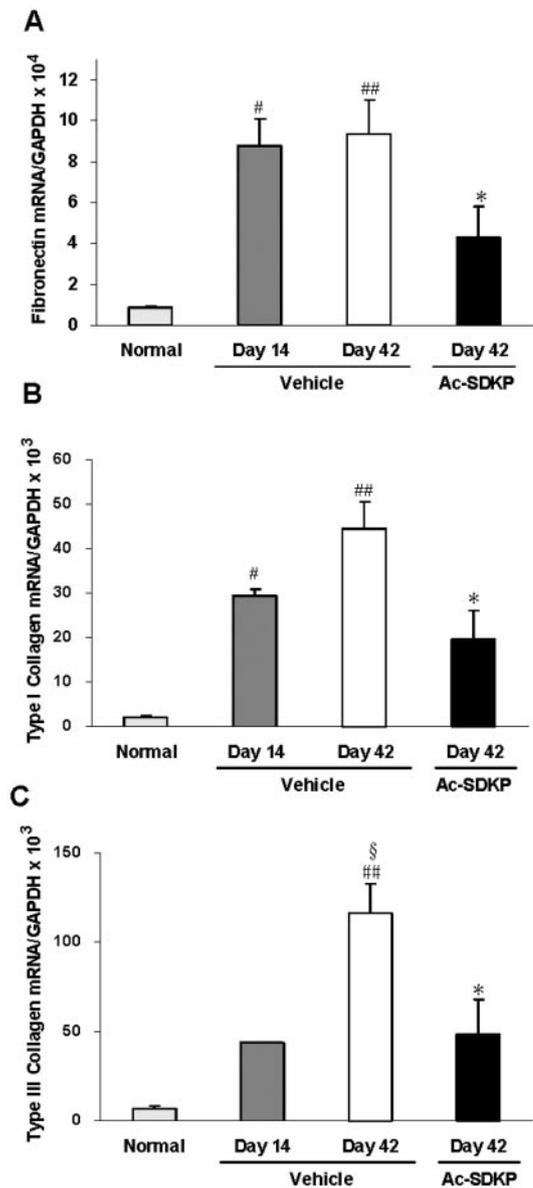
Figure 3. Inhibitory effects of Ac-SDKP on gene expression of extracellular matrix in the anti-GBM nephritis rats. Levels of mRNA encoding fibronectin (A), type I collagen (B), and type III collagen (C) in the kidney cortex were determined by real-time reverse transcription–PCR (RT-PCR) analyses. Each column shows data from normal rats (light gray column), day 14 nephritic rats that were treated with vehicle (dark gray column), day 42 nephritic rats that were treated with vehicle (□), and day 42 nephritic rats that were treated with 1 mg/kg per d Ac-SDKP (■). Each column represents the mean ± SEM of four rats for the normal and day 14 vehicle groups or seven rats for the day 42 vehicle and Ac-SDKP groups. Statistical significance: #$P < 0.05$, ##$P < 0.01$ versus the normal group; §$P < 0.05$ versus day 14 in the nephritic rats by Dunnett test; *$P < 0.05$ versus day 42 in the vehicle group by the t test.

treated group was significantly higher than that in the vehicle group (Figure 1D).

Histologic Injury

In comparison with renal sections from normal rats (Figure 2A), the rats with anti-GBM nephritis showed mild glomerulo-
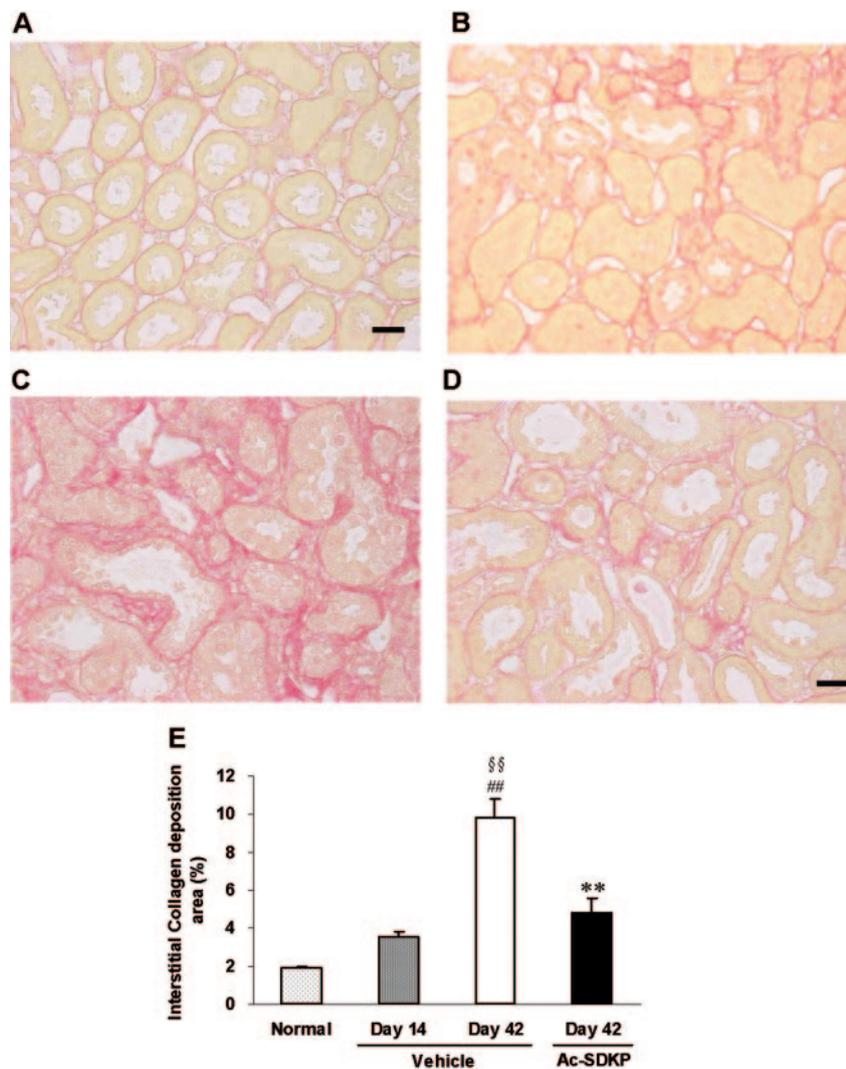
Figure 4. Effects of Ac–SDKP on collagen deposition in the tubulointerstitium of anti-GBM nephritic rats. (A through D) Representative photomicrographs of tubular lesions in renal sections from normal rats (A), day 14 nephritic rats (B), day 42 nephritic rats that were treated with vehicle (C), and day 42 nephritis rats treated with 1 mg/kg per d Ac-SDKP (D). (E) The percentage of the entire field that was stained red was calculated. Each column shows data from normal rats (light gray column), day 14 nephritic rats that were treated with vehicle (dark gray column), day 42 nephritic rats that were treated with vehicle (□), and day 42 nephritic rats that were treated with 1 mg/kg per d Ac-SDKP (■). Each column represents the mean ± SEM of four rats for the normal and day 14 vehicle groups and seven rats for the day 42 vehicle and Ac-SDKP groups. Statistical significance: [##]$P < 0.01$ *versus* normal group, [§§]$P < 0.01$ *versus* day 14 in nephritis rats by Dunnett test; **$P < 0.01$ *versus* day 42 in the vehicle group by the *t* test. Bar = 50 μm.

sclerosis (GSI 0.78 ± 0.06) with cellular crescent formation in almost 50% of the glomeruli on day 14 (Figure 2B). Glomerular lesions in the vehicle-treated rats progressed thereafter, and on day 42, a marked degree of glomerulosclerosis was exhibited (GSI 1.40 ± 0.15; Figure 2C). The glomerulosclerosis was significantly ameliorated by the treatment with Ac-SDKP (GSI 0.71 ± 0.07; Figure 2, D and I). In rats with anti-GBM nephritis, slight tubulointerstitial fibrosis was seen on day 14 (2.99 ± 0.35%; Figure 2F) and interstitial injury showed marked development on day 42 (18.49 ± 1.90%; Figure 2G) compared with normal rats (Figure 2E). Treatment with Ac-SDKP significantly blunted the formation of interstitial fibrosis on day 42 (9.45 ± 1.07%; Figure 2, H and J).

Expression of ECM

Expression of fibronectin mRNA in nephritic kidneys on days 14 and 42 was 10-fold higher than that in normal kidneys; this upregulation was significantly attenuated (54.7% reduction) by Ac-SDKP treatment (Figure 3A). In the vehicle-group, the type I and III collagen mRNA levels were increased by 14- and 6-fold, respectively, on day 14 and further increased to 21- and 17-fold, respectively, on day 42. The upregulation of these genes was also significantly suppressed by Ac-SDKP treatment (55.5 and 58.3% reduction at day 42 compared with the vehicle group; Figure 3, B and C). The deposition of interstitial collagen protein stained with picrosirius red was greater on days 14 (3.6%) and 42 (9.8%) in rats with anti-GBM nephritis relative to

normal rats (1.9% at day 42). Ac-SDKP treatment significantly reduced the amount of collagen deposition (4.8%) on day 42 compared with the vehicle group (Figure 4). Furthermore, Western blot analysis demonstrated that the expression of fibronectin protein was remarkably increased on day 42 in rats with nephritis; Ac-SDKP treatment resulted in a significant inhibition of fibronectin expression compared with the vehicle group (Figure 5).

Levels of TGF-β1 Gene and Protein Expression

The levels of TGF-β1 mRNA obtained from the kidneys of vehicle-treated rats on day 42 were elevated relative to normal rats. Ac-SDKP treatment significantly reduced TGF-β1 gene expression on day 42 relative to vehicle treatment (Figure 6A). Total levels of TGF-β1 protein were increased by nephritis induction and significantly reduced by Ac-SDKP treatment (Figure 6B).

TGF-β Intracellular Signaling

To explore the underlying mechanism of Ac-SDKP activity against renal fibrosis, we used Western blotting to examine the effects of Ac-SDKP treatment on the TGF-β signaling-related molecules Smad2 and Smad7. Compared with the normal rat kidneys, vehicle-treated nephritic kidneys exhibited increased phosphorylation of Smad2. Ac-SDKP treatment resulted in a 44% reduction of Smad2 phosphorylation relative to the vehi-

cle-treated kidneys (Figure 7, A and C). Smad7 protein was moderately expressed in normal kidneys. It is interesting that Smad7 protein expression showed a 50% reduction in nephritic kidneys relative to normal kidneys. Ac-SDKP treatment resulted in significant upregulation of Smad7 expression to a level 3.6-fold higher than that observed in vehicle-treated rats (Figure 7, B and D).

Monocyte/Macrophage Infiltration

ED-1–positive cells were observed only rarely in the glomeruli and the interstitium of normal rats (Figure 8, A and E). In rats with anti-GBM nephritis on day 14, ED-1–positive cells had markedly accumulated into the glomeruli and the tubulointerstitium (Figure 8, B and F). On day 42, the number of ED-1–positive cells had further increased in the tubulointerstitium (Figure 8G); however, the number of ED-1–positive cells tended to be lower in the glomeruli (Figure 8C). In the Ac-SDKP–treated rats, the number of ED-1–positive cells on day 42 was significantly reduced in both the glomeruli (Figure 8, D and I) and tubulointerstitium (Figure 8, H and J) compared with the vehicle-treated rats.

Expression of Inflammation-Related Genes

To elucidate the mechanism by which Ac-SDKP inhibits macrophage infiltration, we evaluated the effects of Ac-SDKP on inflammation-related genes, including monocyte chemoattrac-
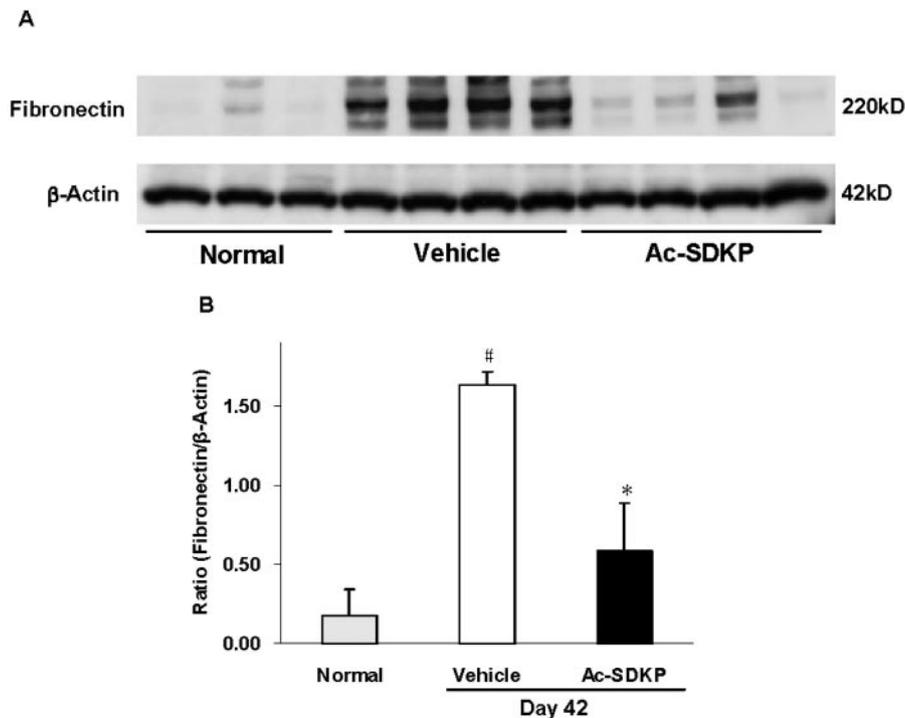
Figure 5. Effects of Ac-SDKP on fibronectin expression in kidneys from anti-GBM nephritis rats. (A) Representative Western blot shows the expression of fibronectin at 220 kD and β-actin as a control in the renal cortex on day 42 in nephritic and normal rats. (B) Densitometric quantification of the corresponding bands was performed using an image analyzer. The data are presented after normalization to β-actin expression. Each column shows data for the normal rats (▨), day 42 nephritic rats that were treated with vehicle (□), and day 42 nephritic rats that were treated with 1 mg/kg per d Ac-SDKP (■). Each column represents the mean ± SEM of three to four samples. Statistical significance is based on the Mann-Whitney U test: #P < 0.05 *versus* the normal group; *P < 0.05 *versus* the vehicle group.
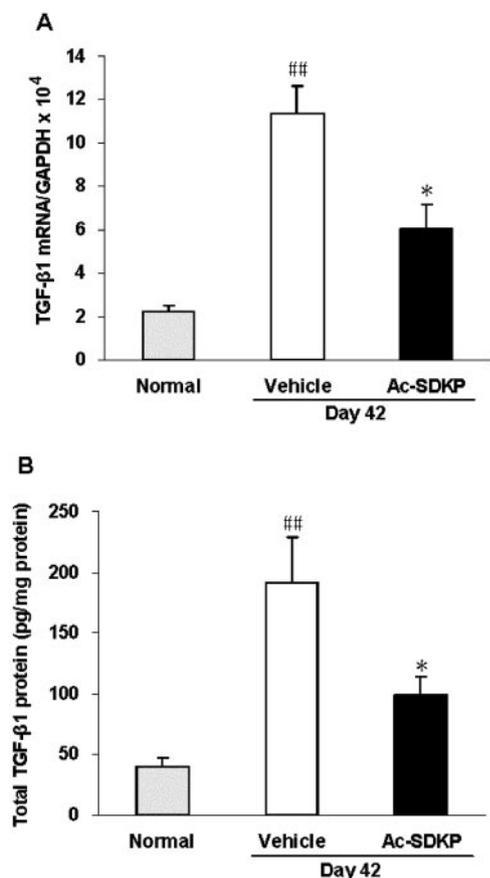
Figure 6. Effects of Ac-SDKP on TGF-β1 gene and protein expression in the kidney cortex of anti-GBM nephritic rats. TGF-β1 gene (A) and protein (B) levels were determined by real-time RT-PCR and ELISA, respectively. Renal cortex tissue was isolated from normal rats and from anti-GBM nephritic rats on day 42. TGF-β1 gene expression and protein levels are presented after normalization to glyceraldehyde-3-phosphate dehydrogenase (GAPDH) or total protein levels in the same sample, respectively. Each column shows data from normal rats (▨), day 42 nephritic rats that were treated with vehicle (□), and day 42 nephritic rats that were treated with 1 mg/kg per d Ac-SDKP (■). Each column represents the mean ± SEM of four rats for the normal group or seven rats for the day 42 vehicle and Ac-SDKP groups. Statistical significance: [##]$P < 0.01$ *versus* the normal group by Dunnett test; *$P < 0.05$ *versus* the vehicle group by the t test.

tant protein-1 (MCP-1), TNF-α, IL-1β, and intercellular adhesion molecule-1 (ICAM-1). The levels of MCP-1, TNF-α, IL-1β and ICAM-1 mRNA were markedly upregulated on day 42 in nephritic kidneys relative to normal kidneys. The alterations in the expression of these genes were significantly suppressed by Ac-SDKP treatment (Figure 9).

Number of Peripheral Leukocytes and the Plasma Concentration of Ac-SDKP

We examined the effects of Ac-SDKP treatment on the number of peripheral leukocytes in nephritic rats. There were no differences in the number of peripheral leukocytes among the three groups (normal group $0.98 \pm 0.03 \times 10^7$ cells/ml; vehicle

group $1.08 \pm 0.07 \times 10^7$ cells/ml; Ac-SDKP group $1.14 \pm 0.09 \times 10^7$ cells/ml).

The plasma concentrations of Ac-SDKP were determined using a commercial EIA kit. The endogenous Ac-SDKP concentration was 1.98 ± 0.16 nM in the vehicle-treated rats. After the subcutaneous administration of 1 mg/kg per d Ac-SDKP for 4 wk, the Ac-SDKP concentration was increased to 36.06 ± 8.35 nM.

Discussion

In this study, we used a rat chronic progressive glomerulonephritis model to investigate the possible efficacy of Ac-SDKP as a novel medicine for the treatment of established kidney disease. Although treatment was not started until 2 wk after nephritis induction, Ac-SDKP significantly suppressed proteinuria and inhibited the progression of renal dysfunction. Histologic analysis showed that the development of the glomerulosclerosis and tubulointerstitial fibrosis was significantly inhibited by Ac-SDKP treatment.

TGF-β is known to play a crucial role in the progression of renal fibrosis in clinical and experimental renal disease (18). It has been reported that the blockade of TGF-β action by overexpressing soluble TGF-β type II receptor ameliorated renal dysfunction and fibrosis in an anti-GBM nephritis model in rats (19). Recent studies have suggested that TGF-β transmits biologic signals from the plasma membrane to the nucleus using Smads as intracellular effector molecules (24,25). After TGF-β binds to its receptors, the activated receptors induce phosphorylation of the receptor-regulated Smad2/3 (R-Smads) proteins, which then associate with a common partner, Smad4. The heterodimers translocate to the nucleus, where they modulate the expression of TGF-β target genes (26). The inhibitory protein, Smad7, is upregulated by some stimuli and acts by occupying the ligand-activated TGF-β type I receptor, interfering with the phosphorylation of R-Smad (27,28). It has been demonstrated that the overexpression of Smad7 by gene transfer ameliorated renal fibrosis in rat *in vivo* models (29,30). In our anti-GBM nephritis model, TGF-β1 mRNA and protein expression was upregulated markedly in the kidney, Smad7 was downregulated, and Smad2 was inversely activated. Recently, it was reported that a mouse model of unilateral ureteral obstruction showed renal fibrosis with a concomitant decrease of Smad7 protein and activation of Smad2 (31). It is likely that the results observed in our model are partially caused by activation of the TGF-β signaling pathway, which can aggravate renal fibrosis, as in the unilateral ureteral obstruction model. To elucidate the mechanism of Ac-SDKP inhibition of renal dysfunction and fibrosis in this nephritis model, we examined the effects of Ac-SDKP on the TGF-β signaling pathway. Pokharel *et al.* (32) reported that Ac-SDKP inhibited the TGF-β–stimulated proliferation of cardiac fibroblasts by inhibiting Smad2 phosphorylation. We also have reported that Ac-SDKP inhibited TGF-β signaling by suppressing Smad2 activation *via* the nuclear export of Smad7 in human mesangial cells (17). Furthermore, Ac-SDKP ameliorated glomerulosclerosis by inhibiting Smad3 activation in diabetic mice (14). In the model used in this study, Ac-SDKP not only reduced TGF-β1
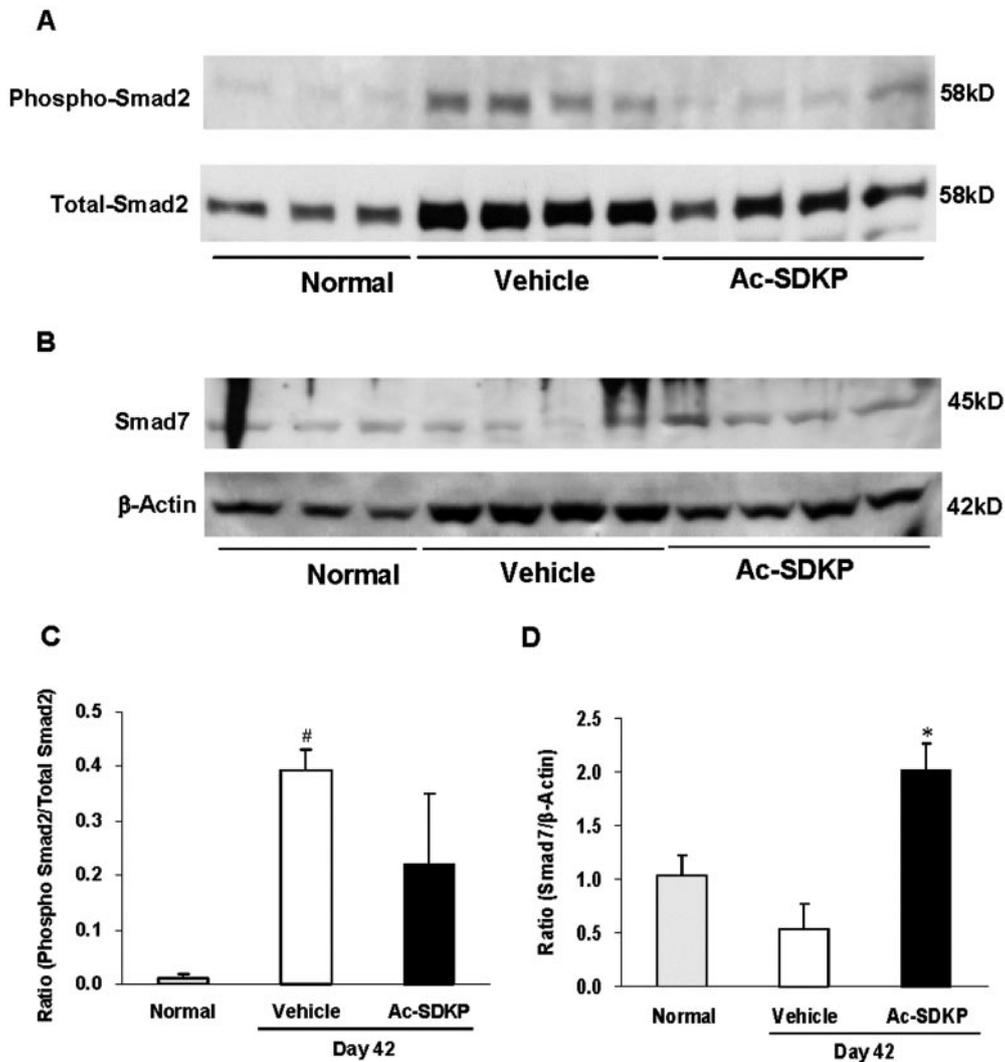
Figure 7. Effects of Ac-SDKP on the phosphorylation of Smad2 and the expression of Smad7 in kidneys from anti-GBM nephritic rats. Representative Western blotting shows the expression of phosphorylated Smad2 and total Smad2 at 58 kD (A) and the expression of Smad7 at 45 kD and β-actin as a control (B). (C and D) Densitometric quantification of the corresponding bands was performed using an image analyzer. The data are presented after normalization to total Smad2 expression or β-actin expression. Each column shows data from normal rats (▒), day 42 nephritic rats that were treated with vehicle (□), and day 42 nephritic rats that were treated with 1 mg/kg per d Ac-SDKP (■). Each column represents the mean ± SEM of three to four samples. Statistical significance is based on the Mann-Whitney *U* test: [#]$P < 0.05$ *versus* the normal group; [*]$P < 0.05$ *versus* the vehicle group.

protein expression but also inhibited Smad2 activation and restored Smad7 protein expression. From these results, we speculate that Ac-SDKP inhibits renal fibrosis *via* blockade of the TGF-β/Smad signal transduction pathway.

In our model, monocytes/macrophages accumulated remarkably into the glomeruli and tubulointerstitium. Ac-SDKP treatment significantly attenuated monocyte/macrophage accumulation and suppressed the expression of mediators of the inflammatory response in the renal tissue. These results led us to speculate that Ac-SDKP inhibits monocyte/macrophage accumulation *via* the suppression of proteins that are involved in the inflammatory response. It has been reported that monocytes/macrophages that infiltrate into the glomeruli and tubulointerstitium may play a pivotal role in the progression of renal fibrosis. Indeed, blockade of monocyte/macrophage ac-

cumulation by anti—MCP-1 antibody has been shown to improve the renal fibrosis in anti-GBM rat nephritis (33,34). Therefore, the antifibrotic action of Ac-SDKP may also be attributed partially to the suppression of monocyte/macrophage accumulation. Furthermore, to assess the possibility that Ac-SDKP–induced attenuation of monocyte/macrophage accumulation into the renal tissue was due to the inhibition of hematopoietic stem cell proliferation, another function of Ac-SDKP, we evaluated the effects of Ac-SDKP on the number of peripheral leukocytes. If Ac-SDKP exerted an inhibitory effect on the hematopoietic stem cell proliferation, then we would predict a reduction in the number of each type of leukocyte, including monocytes, neutrophils, and lymphocytes (35,36). However, in our study, the number of total leukocytes was not decreased by Ac-SDKP treatment. Therefore, we speculate that Ac-SDKP did
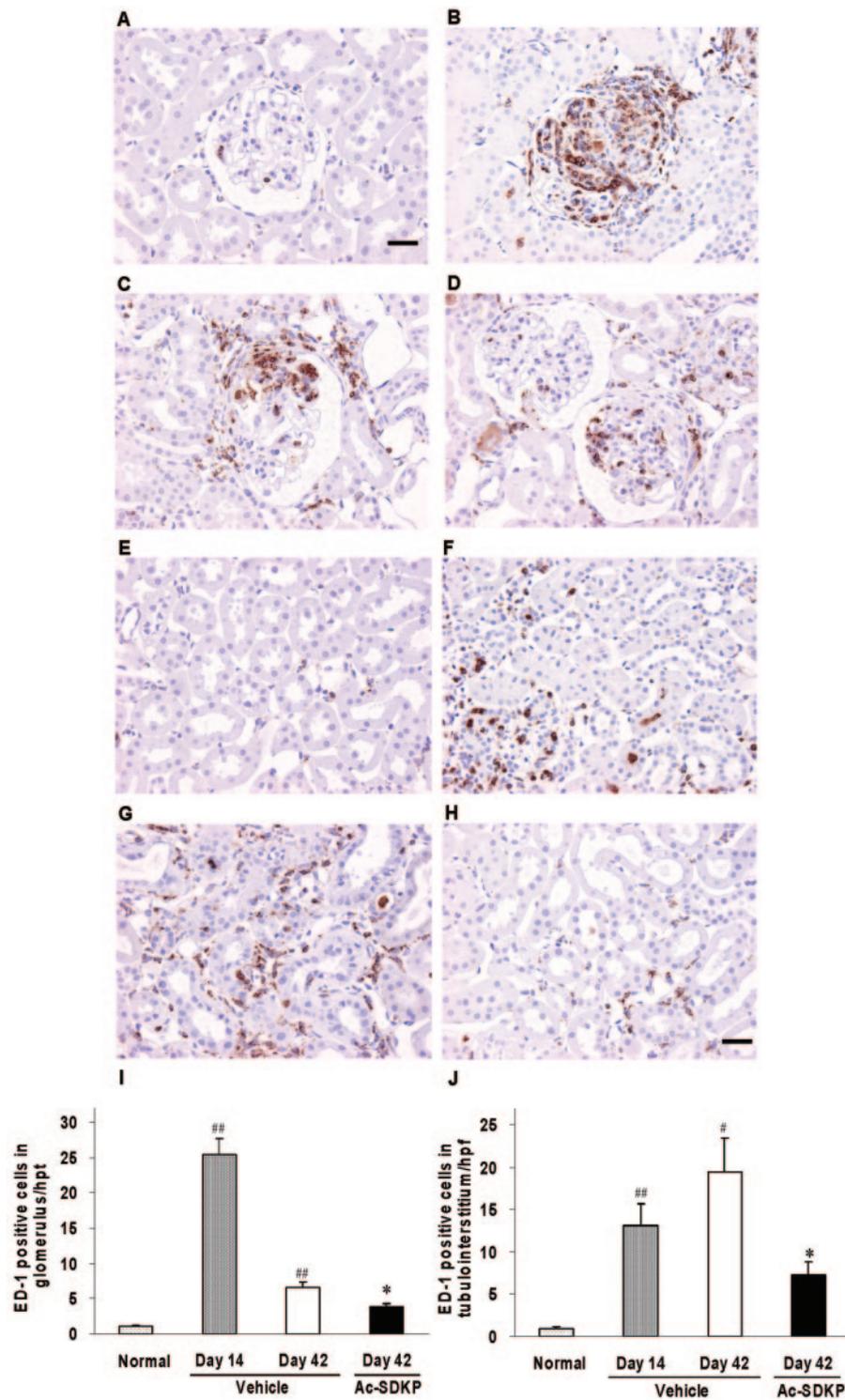
Figure 8. Effects of Ac-SDKP on ED-1–positive monocyte/macrophage infiltration into the glomerulus and tubulointerstitium. (A through D) Representative photomicrographs of glomerular lesions in renal sections from normal rats (A), day 14 nephritic rats (B), day 42 nephritic rats that were treated with vehicle (C), and day 42 nephritic rats that were treated with 1 mg/kg per d Ac-SDKP (D). (E through H) Representative photomicrographs of tubular lesions in renal sections from normal rats (E), day 14 nephritic rats (F), day 42 nephritic rats that were treated with vehicle (G), and day 42 nephritic rats that were treated with Ac-SDKP (H). Quantification of monocyte/macrophage infiltration into the glomerulus (I) and tubulointerstitium (J) was evaluated by counting the number of ED-1–positive cells. Each column shows data from normal rats (light gray column), day 14 nephritic rats that were treated with vehicle (dark gray column), day 42 nephritic rats that were treated with vehicle (□), and day 42 nephritic rats that were treated with 1 mg/kg per d Ac-SDKP (■). Each column represents the mean ± SEM of four rats for the normal and day 14 vehicle groups or seven rats for the day 42 vehicle and Ac-SDKP groups. Statistical significance: [#]$P < 0.05$, [##]$P < 0.01$ *versus* the normal group by Dunnett test; *$P < 0.05$ *versus* day 42 in the vehicle group by the *t* test. Bar = 30 μm.
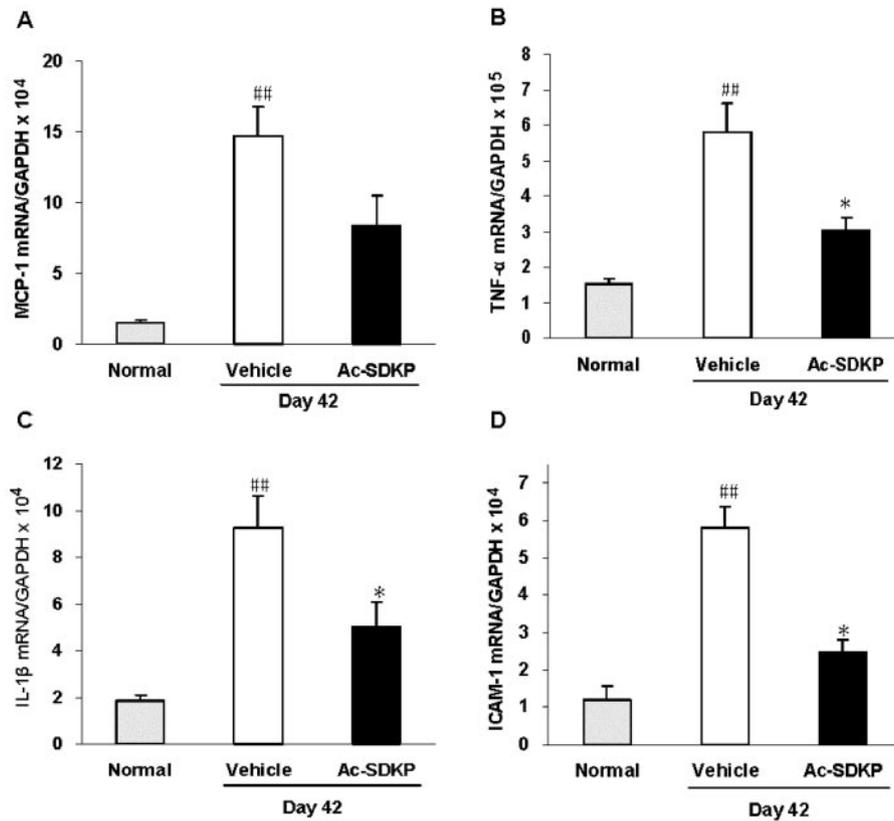
Figure 9. Inhibitory effect of Ac-SDKP on the expression of genes that are involved in the inflammatory response in anti-GBM nephritic rats. The mRNA levels of monocyte chemoattractant protein-1 (MCP-1; A), TNF-α (B), IL-1β (C), and intercellular adhesion molecule-1 (ICAM-1; D) were determined by real-time RT-PCR analyses. Renal cortex tissue was isolated from anti-GBM nephritic rats on day 42. All data are presented after normalization to the level of GAPDH in the same sample. Each column shows data from normal rats (▨), day 42 nephritic rats that were treated with vehicle (□), and day 42 nephritic rats that were treated with 1 mg/kg per d Ac-SDKP (■). Each column represents the mean ± SEM of four rats for the normal group or seven rats for the day 42 vehicle and Ac-SDKP groups. Statistical significance: $^{\#\#}P < 0.01$ *versus* the normal group by Dunnett test; $^{*}P < 0.05$ *versus* the vehicle group by the *t* test.

not affect stem cell proliferation and that the numbers of circulating monocytes in Ac-SDKP– and vehicle-treated rats were similar. It follows that Ac-SDKP may have inhibited monocyte infiltration without changing the number of monocytes in the peripheral blood.

We and others have reported that a 10- to 100-nM concentration of Ac-SDKP is effective against TGF-β signal transduction and expression of extracellular matrix *in vitro* (17,32). In this study, the plasma Ac-SDKP concentration in the Ac-SDKP–treated group was 36 nM, 18 times greater than the endogenous levels and within the range of the effective concentrations in the *in vitro* experiments.

Conclusion

We have demonstrated for the first time that Ac-SDKP significantly ameliorated the progression of renal dysfunction and fibrosis, after the establishment of glomerulonephritis. Thus, Ac-SDKP treatment may represent a novel therapeutic strategy for halting the progression of renal disease.

References

1. Blantz RC: Reflections on the past, transitions to the future: The American Society of nephrology. *J Am Soc Nephrol* 14: 1695–1703, 2003
2. Burkart JM, Pereira BJ, Parker TF 3rd: Strategies for influencing outcomes in pre-ESRD and ESRD patients. *J Am Soc Nephrol* 9: S2–S3, 1998
3. Port FK, Fenton SSA, Mazzuchi N: ESRD throughout the world: Morbidity, mortality and quality of life. *Kidney Int* 57: S1–S2, 2000
4. Remuzzi G, Bertani T: Pathophysiology of progressive nephropathies. *N Engl J Med* 339: 1448–1456, 1998
5. Eddy AA: Molecular insights into renal interstitial fibrosis. *J Am Soc Nephrol* 7: 2495–2508, 1996
6. Brenner BM: Remission of renal disease: Recounting the challenge, acquiring the goal. *J Clin Invest* 110: 1753–1758, 2002
7. Hebert LA, Wilmer WA, Falkenhain ME: Ladson-Wofford SE, Nahman NS, Rovin BH: Renoprotection: One or many therapies? *Kidney Int* 59: 1211–1226, 2001
8. Peters H, Border WA, Noble NA: Targeting TGF-beta over-

expression in renal disease: Maximizing the antifibrotic action of angiotensin II blockade. *Kidney Int* 54: 1570–1580, 1998

9. Wdzieczak-Bakala J, Fache MP, Lenfant M, Frindel E, Sainteny F: Ac-SDKP, an inhibitor of CFU-S proliferation, is synthesized in mice under steady-state conditions and secreted by bone marrow in long-term culture. *Leukemia* 4: 235–237, 1990

10. Azizi M, Rousseau A, Ezan E, Guyene T-T, Michelet S, Grognet J-M, Lenfant M, Corvol P, Menard J: Acute angiotensin-converting enzyme inhibition increases the plasma level of the natural stem cell regulator N-acetyl-seryl-aspartyl-lysyl-proline. *J Clin Invest* 97: 839–844, 1996

11. Peng H, Carretero O, Raij L, Yang F, Kapke A, Rhaleb NE: Anti-fibrotic effects of N-acetyl-seryl-aspartyl-lysyl-proline on the heart and kidney in aldosterone-salt hypertensive rats. *Hypertension* 34: 794–800, 2001

12. Rhaleb NE, Peng H, Yang XP, Liu YH, Mehta D, Ezan E, Carretero OA: Long-term effect of N-acetyl-seryl-aspartyl-lysyl-proline on left ventricular collagen deposition in rats with 2-kidney, 1-clip hypertension. *Circulation* 103: 3136–3141, 2001

13. Peng F, Yang XP, Liu YH, Xu J, Cingolani O, Rhaleb NE, Carretero OA: Ac-SDKP reverses inflammation and fibrosis in rats with heart failure after myocardial infarction. *Hypertension* 43: 229–236, 2004

14. Shibuya K, Kanasaki K, Isono M, Sato H, Omata M, Sugimoto T, Araki S, Isshiki K, Kashiwagi A, Haneda M, Koya D: N-acetyl-seryl-aspartyl-lysyl-proline prevents renal insufficiency and mesangial matrix expansion in diabetic db/db mice. *Diabetes* 54: 838–845, 2005

15. Iwamoto N, Xano HJ, Yoshioka T, Shiraga H, Hitta K, Muraki T, Ito K: Acetyl-seryl-aspartyl-lysyl-proline is a novel natural cell cycle regulator of renal cells. *Life Sci* 66: PL221–PL226, 2000

16. Rhaleb N, Peng H, Harding P, Tayeh M, LaPointe M, Carretero O: Effect of N-acetyl-seryl-aspartyl-lysyl-proline on DNA and collagen synthesis in rat cardiac fibroblasts. *Hypertension* 37: 827–832, 2001

17. Kanasaki K, Koya D, Sugimoto T, Isono M, Kashiwagi A, Haneda M: N-Acetyl-seryl-aspartyl-lysyl-proline inhibits TGF-beta-mediated plasminogen activator inhibitor-1 expression via inhibition of Smad pathway in human mesangial cells. *J Am Soc Nephrol* 14: 863–872, 2003

18. Border WA, Noble NA: Mechanisms of disease: Transforming growth factor beta in tissue fibrosis. *N Engl J Med* 331: 1286–1292, 1994

19. Zhou A, Ueno H, Shimomura M, Tanaka R, Shirakawa T, Nakamura H, Matsuo M, Iijima K: Blockade of TGF-beta action ameliorates renal dysfunction and histologic progression in anti-GBM nephritis. *Kidney Int* 64: 92–101, 2003

20. Taniguchi H, Nagamatsu T, Kojima R, Ito M, Suzuki Y: Marked antinephritic action and less adverse effects of methylprednisolone suleptanate by intermittent administration in rats. *Jpn J Pharmacol* 64: 79–88, 1994

21. Kingsbury FB, Clark CP, Williams G, Post AL: The rapid determination of albumin in urine. *J Lab Clin Med* 11: 981–989, 1926

22. De Boer E, Navis G, Tiebosch AT, De Jong PE, De Zeeuw D: Systemic factors are involved in the pathogenesis of proteinuria-induced glomerulosclerosis in Adriamycin nephrotic rats. *J Am Soc Nephrol* 10: 2359–2366, 1999

23. Isshiki K, Haneda M, Koya D, Maeda S, Sugimoto T, Kikkawa R: Thiazolidinedione compounds ameliorate glomerular dysfunction independent of their insulin-sensitizing action in diabetic rats. *Diabetes* 49: 1022–1032, 2000

24. Miyazono K: TGF-beta signal by Smad proteins. *Cytokine Growth Factor Rev* 11: 15–22, 2000

25. Heldin C, Miyazono K, ten Dijke P: TGF-beta signaling from cell membrane to nucleus through SMAD proteins. *Nature* 390: 465–471, 1997

26. Wrana J, Attisano L, Carcamo J, Zentella A, Doody J, Laiho M, Wang X, Massague J: TGF-beta signals through a heteromeric protein kinase receptor complex. *Cell* 71: 1003–1014, 1992

27. Miyazono K: Positive and negative regulation of TGF-beta signaling. *J Cell Sci* 113: 1101–1109, 2000

28. Kavsak P, Rasmussen RK, Causing CG, Bonni S, Zhu H, Thomsen GH, Wrana JL: Smad7 binds to Smurf2 to form an E3 ubiquitin ligase that targets the TGF-beta receptor for degradation. *Mol Cell* 6: 1365–1375, 2000

29. Terada Y, Hanada S, Nakao A, Kuwahara M, Sakai S, Marumo F: Gene transfer of Smad7 using electroporation of adenovirus prevents renal fibrosis in post-obstructed kidney. *Kidney Int* 61[Suppl 1]: S94–S98, 2002

30. Lan HY, Mu W, Tomita N, Huang XR, Li JH, Zhu HJ, Morishita R, Johnson RJ: Inhibition of renal fibrosis by gene transfer of inducible Smad7 using ultrasound-microbubble system in rat UUO model. *J Am Soc Nephrol* 14: 1535–1548, 2003

31. Fukasawa H, Yamamoto T, Togawa A, Ohashi N, Fujigaki Y, Oda T, Uchida C, Kitagawa K, Hattori T, Suzuki S, Kitagawa M, Hishida A: Down-regulation of Smad7 expression by ubiquitin-dependent degradation contributes to renal fibrosis in obstructive nephropathy in mice. *Proc Natl Acad Sci U S A* 101: 8687–8692, 2004

32. Pokharel S, Rasoul S, Roks AJ, van Leeuwen RE, van Luyn MJ, Deelman LE, Smits JF, Carretero O, van Gilst WH, Pinto YM: N-acetyl-Ser-Asp-Lys-Pro inhibits phosphorylation of Smad2 in cardiac fibroblasts. *Hypertension* 40: 155–161, 2002

33. Wada T, Yokoyama H, Furuichi K, Kobayashi KI, Harada K, Naruto M, Su SB, Akiyama M, Mukaida N, Matsushima K: Intervention of crescentic glomerulonephritis by antibodies to monocyte chemotactic and activating factor (MCAF/MCP-1). *FASEB J* 10: 1418–1425, 1996

34. Fujinaka H, Yamamoto T, Takeya M, Feng L, Kawasaki K, Yaoita E, Kondo D, Wilson CB, Uchiyama M, Kihara I: Suppression of anti-glomerular basement membrane nephritis by administration of anti-monocyte chemoattractant protein-1 antibody in WKY rats. *J Am Soc Nephrol* 8: 1174–1178, 1997

35. Volkov L, Quere P, Coudert F, Comte L, Antipov Y, Praloran V: The tetrapeptide AcSDKP, a negative regulator of cell cycle entry, inhibits the proliferation of human and chicken lymphocytes. *Cell Immunol* 168: 302–306, 1996

36. Gaudron S, Grillon C, Thierry J, Riches A, Wierenga PK, Wdzieczak-Bakala J: In vitro effect of acetyl-N-Ser-Asp-Lys-Pro (AcSDKP) analogs resistant to angiotensin I-converting enzyme on hematopoietic stem cell and progenitor cell proliferation. *Stem Cells* 17: 100–106, 1999